Journal of Alloys and Compounds 794 (2019) 435–442

Contents lists available at ScienceDirect

Journal of Alloys and Compounds

journal homepage: http://www.elsevier.com/locate/jalcom

Effect of Zn on the grain boundary precipitates and resulting alkaline etching of recycled Al-Mg-Si-Cu alloys

Alexander Lutz [a, *], Loïc Malet [b], Jean Dille [c], Luiz Henrique de Almeida [c], Linsey Lapeire [d], Kim Verbeken [d], Stéphane Godet [b], Herman Terryn [a], Iris De Graeve [a]

[a] Group of Electrochemical and Surface Engineering, Department of Materials and Chemistry, Vrije Universiteit Brussel, Belgium
[b] 4MAT, Université Libre de Bruxelles, Belgium
[c] Department of Metallurgical Engineering and Materials, Universidade Federal do Rio de Janeiro, Brazil
[d] Department of Materials, Textiles and Chemical Engineering, Ghent University, Belgium

ARTICLE INFO

Article history:
Received 4 October 2018
Received in revised form
16 April 2019
Accepted 24 April 2019
Available online 28 April 2019

Keywords:
Aluminum (Al-Mg-Si) alloy
Preferential grain etching
Etching mechanism
Zinc
Precipitates
TEM EDX

ABSTRACT

The Zinc level in many 6000 Al alloys (Al-Mg-Si-type) was set to a maximum of 0.03 wt% as common industrial practice. Concentrations above 0.03 wt% can modify the alkaline etching mechanism causing the surface to go from a desired smooth look associated with a grain boundary attack (GBA), into an undesired speckled appearance due to preferential grain etching (PGE), visible after anodizing. This significantly limits the ambition of reducing the carbon footprint of Aluminum by increasing the amount of recycled material in the production process. Because Cu has been reported to counteract this negative effect of Zn, the present study is dedicated to contribute to the understanding of this interaction and is focused on Zn and Cu in peak aged AlMgSi alloys. The chemical composition of the various precipitates formed in two Al6063 alloys was studied by means of TEM and EDX, whereby Zn was found in the Q phase (AlMgSiCu) grain boundary precipitates. Two alloys, with different content of Cu and Zn were studied. The Zn/Cu ratio in the bulk was similar for both alloys, but the level of Zn in the Cu containing Q particles in the grain boundaries was different. The increased Zn concentration in Q phase precipitates is believed to decrease the potential of the precipitates with respect to the surrounding matrix. Thus, the Cu/Zn ratio in these alloys is extremely important as it defines the potential differences that in turn cause either GBA or PGE.

1. Introduction

The 6000 Aluminum alloy series (AlMgSi alloys) have generally a good corrosion performance and good mechanical properties. They are extrudable, well formable and can be precipitation hardened by a suitable heat treatment [1]. During this hardening process, they form metastable nano-precipitates of the MgSi type. Generally, the precipitation sequence of these hardening particles is thought to be supersaturated solid solution (SSSS)→ atomic clusters → Guinier-Preston (GP) zones → β″ (Mg_5Si_6) [2] → β′, U1, U2 → β (Mg_2Si) [3–5]. Alloying elements can disturb the structural ordering, the amount and the length of these precipitates and change the properties of these alloys [6]. If Cu is present in the alloy, Q′ and Q precipitates can form and replace the β′ and β phases, respectively [7–12]. Cu additions increase the hardness by refining the MgSi precipitates [13,14]. Though, Cu also increases the intergranular corrosion (IGC) sensitivity because of Cu segregation at the grain boundaries and the formation of local cathodes [15,16].

One effect of recycling is that certain elements accumulate in the alloys. One such element is Zn which has a relatively high solubility in aluminum and is difficult to remove during scrap melting and recycling. Saito et al. did not identify any Zn containing precipitates in Al-Mg-Si alloys up to concentrations of 0.11 wt% Zn. Only at 1 wt% Zn in a Cu-free Al-Mg-Si alloy, they show that Zn forms a continuous thin film at the grain boundaries [17]. However, already more than 0.03 wt% Zn in Al6060 is generally depreciated due to an undesired surface appearance after alkaline pretreatment [18]. Contrary to the smooth matte finish of grain boundary etching at low Zn levels in 6000 alloys, a spangling surface finish is obtained after alkaline etching Zn enriched 6000 alloys. The reason for this appearance is preferential grain etching (PGE) in alkaline solutions that is still visible after anodizing. Grains oriented in the ⟨111⟩//ND

* Corresponding author.
E-mail address: alexander.lutz@vub.ac.be (A. Lutz).

https://doi.org/10.1016/j.jallcom.2019.04.259
0925-8388/

direction (i.e. parallel to the normal direction) are etched the fastest, ⟨110⟩//ND oriented grains less and ⟨100⟩//ND oriented grain the least. Koroleva et al. motivate this behavior for pure aluminum with different inter-atomic distances in the various grains [19]. Several groups have investigated the PGE effect. The general conclusion is that a thin Zn enriched layer is formed on the Aluminum surface during the alkaline etching process which influences the etching behavior. Though, the nature of this layer is not well defined [20–24]. To avoid this phenomenon the zinc level in many 6000 Al alloys was set to a maximum of 0.03 wt% as common industrial practice.

This, however, significantly limits the ambition of reducing the carbon footprint of Aluminum by increasing the amount of recycled material in the production process. To maintain the desired composition of aluminum alloys made from scrap - staying within the permitted alloying element levels -, high purity aluminum is added to the recycling process. Needless to mention that the enrichment of alloying elements like Zn is thus an issue for the recycling progress; understanding and solving this effect of Zn on 6000 Al series alloys would allow more scrap to be used as raw material and an eco-friendlier production of aluminum.

Several somehow contradicting observations point out that PGE and its causes are not fully understood yet. Firstly, this phenomenon does not appear in the 7xxx Al series, which has a much higher amount of Zn (up to several percent), but where hardening precipitates of the $MgZn_2$ type are formed instead of the Mg_2Si precipitates in the 6000 series. Secondly, several authors point towards an effect of Zn dissolved in the etching bath which forms a thin layer on the surface of the aluminum alloy [23,24]. Thirdly, various authors also show that the zinc level in 6000 Al alloys is not the only reason for PGE. The Zn content in the etching bath as well as effects of thermal and mechanical treatment can play a similar role [21,23,25–28]. Fourthly, PGE can be avoided in Zn rich 6000 type alloys if the Cu content of the alloys is at a similar level (approximately 1:1) [29,30]. The maximum Zn level above which PGE occurs, is thus not a constant value, but varies from alloy to alloy. However, there is no common sense yet on what exactly is happening at the Al surface while preferential grain etching is taking place in alkaline solutions and what is the exact effect of Zn on the etching mechanism or even on the structure of the 6000 alloys.

Therefore, the main objective of this study was to investigate the effect of chemical composition differences of two 6063 Al alloys with respect to their different mechanisms of alkaline etching. The authors focused on the interaction between Zn and Cu at approximately the same Zn/Cu ratios. Variation of this ratio might cause a different etching mechanism as described elsewhere [29,30].

2. Experimental

Two 6063 alloys were investigated with the chemical compositions as given in Table 1.

The Zn content of 6063 alloy (0.03 wt%) corresponds to the upper industrial limit whereas the Zn content of 6063Z alloy (0.13 wt%) is well above this level. The amount of Cu in the 6063Z sample is adapted to keep approximatively the same Cu/Zn ratio (roughly two third) as in the 6063 sample. The billets were heat treated at 580 °C for 4 h to homogenize the microstructure before extrusion, assure the uniform distribution of alloying elements in the matrix and dissolve the Mg_2Si particles that formed during casting [27]. Afterwards, the alloys were reheated to 480 °C and extruded at the speed of 27.5 m/min in an industrial press. Subsequently, the profiles were cooled by forced air and artificially aged to T5 (185 °C for 5 h).

Table 1
Chemical compositions of the two investigated alloys in wt%.

Sample name	Si	Mg	Fe	Mn	Cr	Cu	Zn	Al
6063	0.54	0.50	0.26	0.05	0.01	0.02	0.03	to 100 wt%
6063Z	0.37	0.50	0.26	0.08	0.01	0.08	0.13	to 100 wt%

The samples were degreased in acetone, followed by alkaline etching in 50 g/L NaOH for 13 min at 60 °C, rinsing with milliQ water, acid desmutting with 10 vol% HNO_3 at room temperature for 1 min and rinsing again with milliQ water and finally with ethanol. The solutions were prepared using milliQ water.

SEM imaging was performed on a FEI Quanta 200 3D scanning electron microscope. The TEM investigations were conducted using a ChemiSTEM FEI Titan 80–200 field emission gun scanning transmission electron microscope, equipped with 4 EDX detectors and operating at 200 kV. The thin foils were prepared by twin-jet electropolishing (Struers Tenupol 5) in a chemical solution of 75% methanol and 25% nitric acid at −15 °C and 12 V.

3. Results

Fig. 1 shows that 6063 and 6063Z alloys have different visual aspects after the same alkaline etching procedure. A smooth surface finish is obtained for alloy 6063 whereas a spangling surface finish is obtained for alloy 6063Z.

SEM imaging of etched surfaces, shown in Fig. 2, reveals that these different visual aspects correspond to different surface topography. 6063 surface show typical grain boundary attack (marked with arrows in Fig. 2a). The most prominent feature of 6063Z surface is the preferential attack of the interior of the grains (marked with arrows in Fig. 2b).

The TEM bright-field images in Fig. 3a and b shows the formation of needle-like nanometer sized β'' precipitates in 6063 and 6063Z samples in peak aged conditions, respectively. The morphology, size and density of those precipitates are very similar in both alloys, suggesting that Zn addition has no significant influence on β'' precipitation. In addition to the precipitation hardening phase β'', both alloys also contain coarse slightly spheroidal particles (Fig. 3c) inside the grain and elongated grain boundary precipitates (Fig. 3d).

The electron diffraction pattern indexation shown in Fig. 4a permits to identify the coarse precipitates as the α–Al(Fe,Mn)Si phase. α phase has a body-centered structure with a lattice parameter a = 1.26 nm. This phase already exists before aging and is considered as a stable phase in the Al-Fe-Mn-Si quaternary system. Its composition can vary, but is most commonly mentioned as $Al_{12}(Fe,Mn)_3Si$ [31]. The electron diffraction pattern indexation shown in Fig. 4b identifies the grain boundary precipitates as Q phase ($Cu_2Mg_8Si_6Al_5$). The crystallographic structure of Q phase belongs to the hexagonal system with lattice parameters a = 1.04 nm and c = 0.402 nm [31].

Fig. 5a shows the high angle annular dark field (HAADF) STEM image of a 6063Z region containing β'' precipitates. Fig. 5b–f give the corresponding elemental EDX maps. EDX analysis reveals that the β'' precipitates contain Mg and Si and no enrichment of Cu or Zn is detected.

Fig. 6 shows the EDX linescan across an α–Al(Fe,Mn)Si particle along the green line. The composition profiles confirm that the α particle contains Al, Si, Fe and Mn with a high Fe/Mn ratio. A small amount of Cu is also detected but, on the other hand, α–Al(Fe,Mn)Si is Mg and Zn free.

Grain boundary Q precipitates are observed in both 6063 and 6063Z peak aged alloys. Fig. 7 shows an EDX mapping of a grain boundary region in 6063Z alloy. The elemental EDX maps reveal

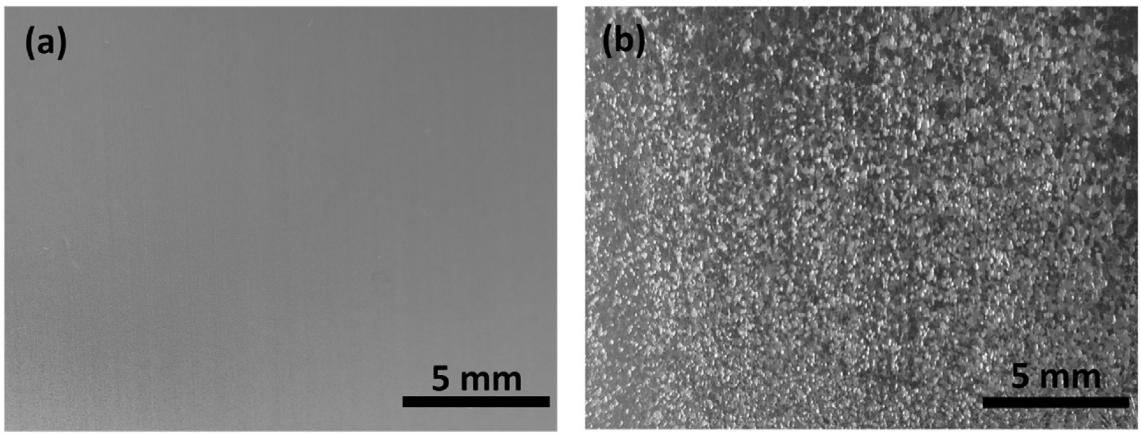

Fig. 1. Visual aspect of (a) 6063 and (b) 6063Z alloys after alkaline etching.

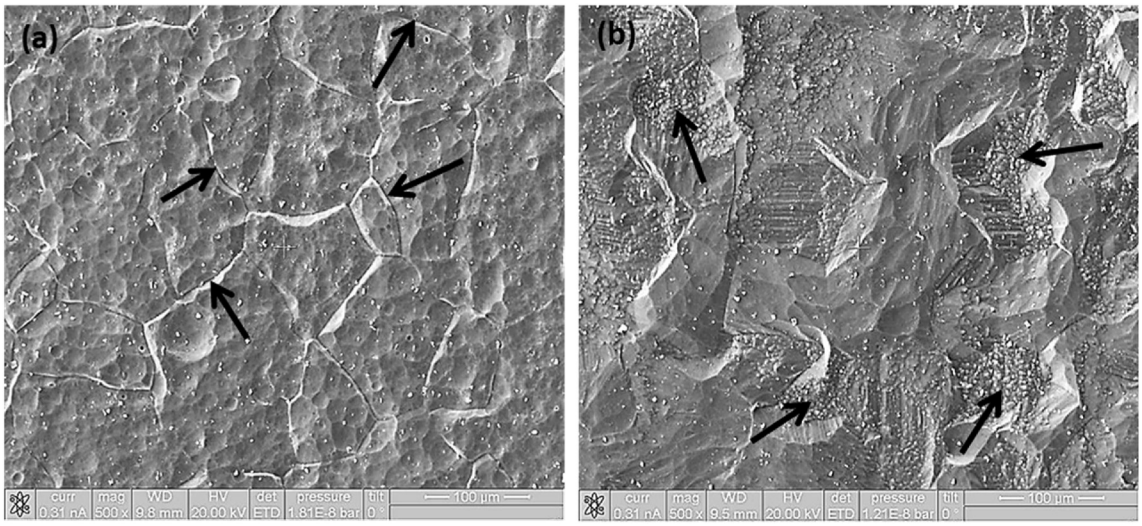

Fig. 2. Surface secondary electron images of 6063 (a) and 6063Z (b) alloys after alkaline etching.

that those grain boundary precipitates are identified as Q phase according to the Q phase determination by electron diffraction. Fig. 7 (e) proves the presence of Zn in these grain boundary Q precipitates. Although a Zn enrichment is observed in the precipitates, there is no continuous film of Cu nor of Zn detected at the grain boundary.

A similar grain boundary region was also studied in 6063 sample, leading to the same conclusion. Fig. 8 compares the EDX spectrum of a grain boundary Q phase precipitate in 6063 and in 6063Z, respectively. It clearly indicates that the Zn/Cu ratio is much higher in 6063Z than in 6063 grain boundary Q phase precipitates.

4. Discussion

The alkaline etching behavior of the two variants of 6063 aluminum alloy is clearly different. The 6063 alloy with a lower Zn content (0.03 wt%) is preferentially attacked at grain boundaries, whereas the 6063Z alloy with a higher Zn content (0.13 wt%) shows a preferential attack of certain grains.

The two alloys were processed in the same way and are peak aged in the same conditions (5 h at 185 °C). For this reason, it can be assumed that their different etching behaviors are related to their different chemical compositions. These chemical compositions are summarized in Table 1.

Although the elemental composition of the two investigated alloys is not the same for all other elements than Zn and Cu, the differences can be neglected for the effects investigated in this paper. Several authors showed that the Mg/Si ratio can be varied in a broad range, still leading to the same precipitation sequence [32,33]. Indeed, the comparison of Fig. 3a and b does not indicate any significant difference in morphology, size and density for nanometer sized β'' precipitates between 6063 and 6063Z alloys, having different Mg/Si ratio. Mn was only found in coarse α–Al(Fe,Mn)Si precipitates existing in both alloys. According to Hatch [31], the Fe/Mn atomic ratio can vary over a very wide range in these precipitates.

To understand the influence of Zn and Cu on the two alloys and their alkaline etching behavior TEM EDX analysis was carried out on thin foils of 6063 and 6063Z samples. The results reveal, that at these concentrations and after peak aging, Cu practically only forms Q-phase precipitates at the grain boundaries. These grain boundaries precipitates are present in both alloys after peak aging. To our knowledge, it is the first time that Zn was found concentrated in precipitates in 6000 alloys and especially in the Q phase grain boundary precipitates.

Concerning the effect of Zn and Cu in such alloys, it is well

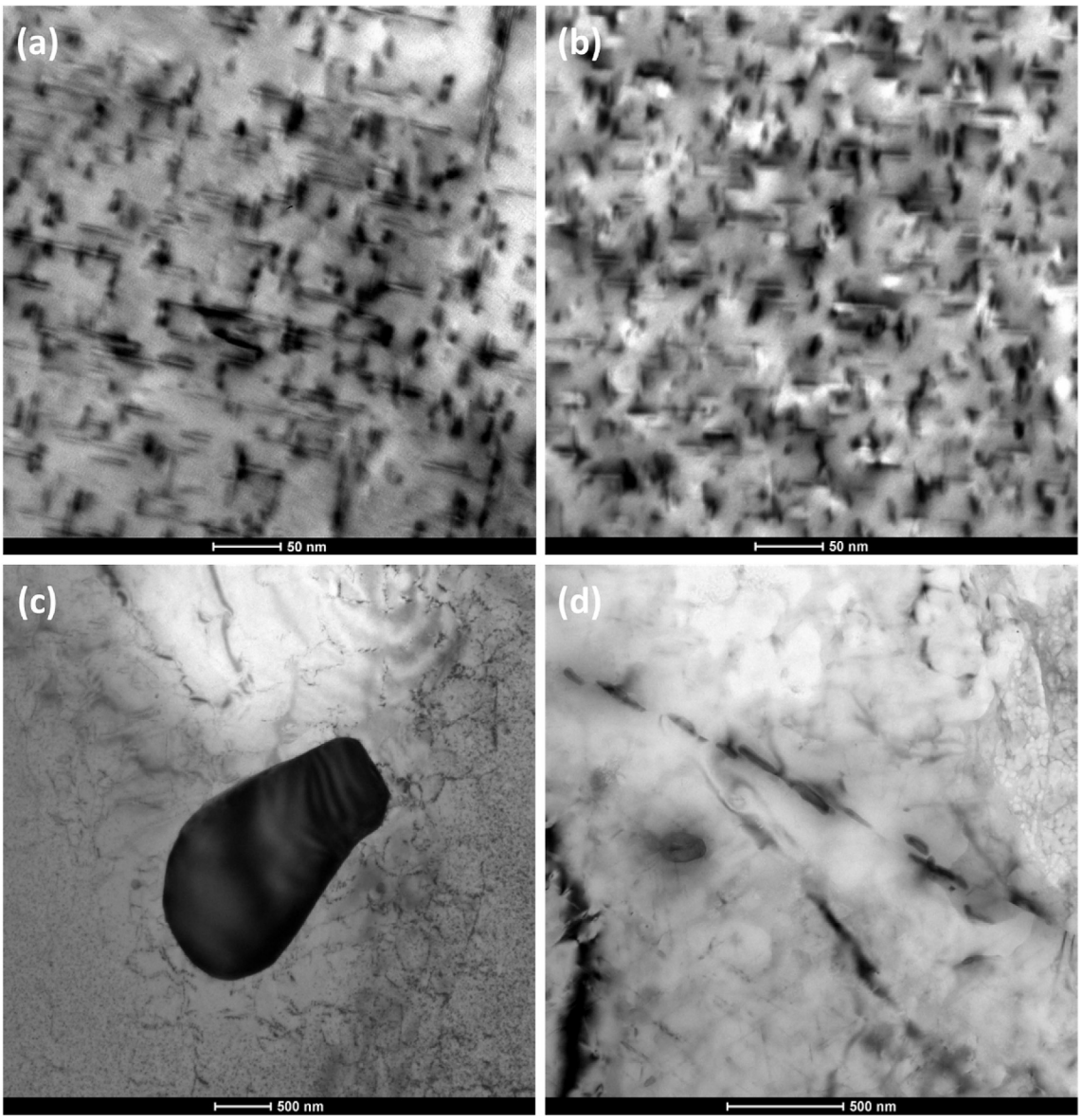

Fig. 3. Bright-field TEM image of β'' precipitates in 6063 (a), β'' precipitates in 6063Z (b), spheroidal precipitate in 6063Z (c) and grain boundary precipitates in 6063Z (d).

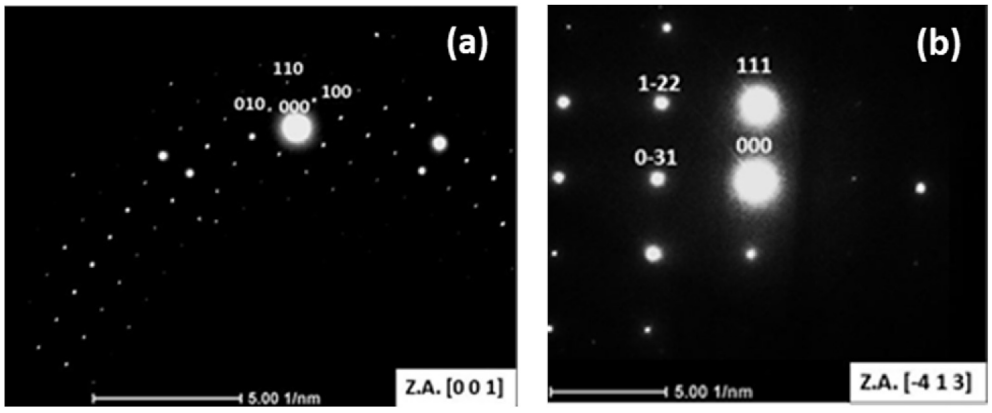

Fig. 4. Electron diffraction pattern of coarse particle (a) and grain boundary precipitate (b) in 6063Z sample peak aged at 185 °C for 5 h.

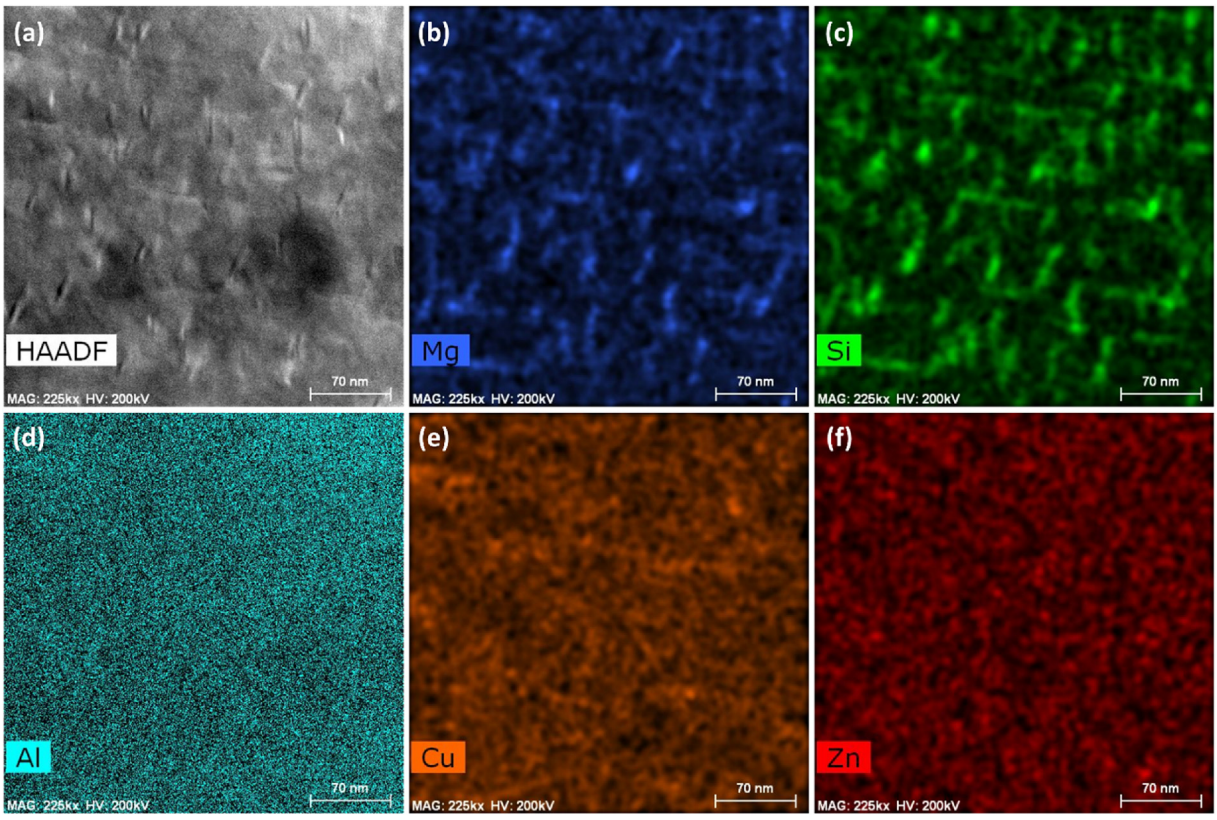

Fig. 5. STEM-HAADF image (a) and EDX elemental mappings (b to f) from 6063Z sample peak aged at 185 °C for 5 h.

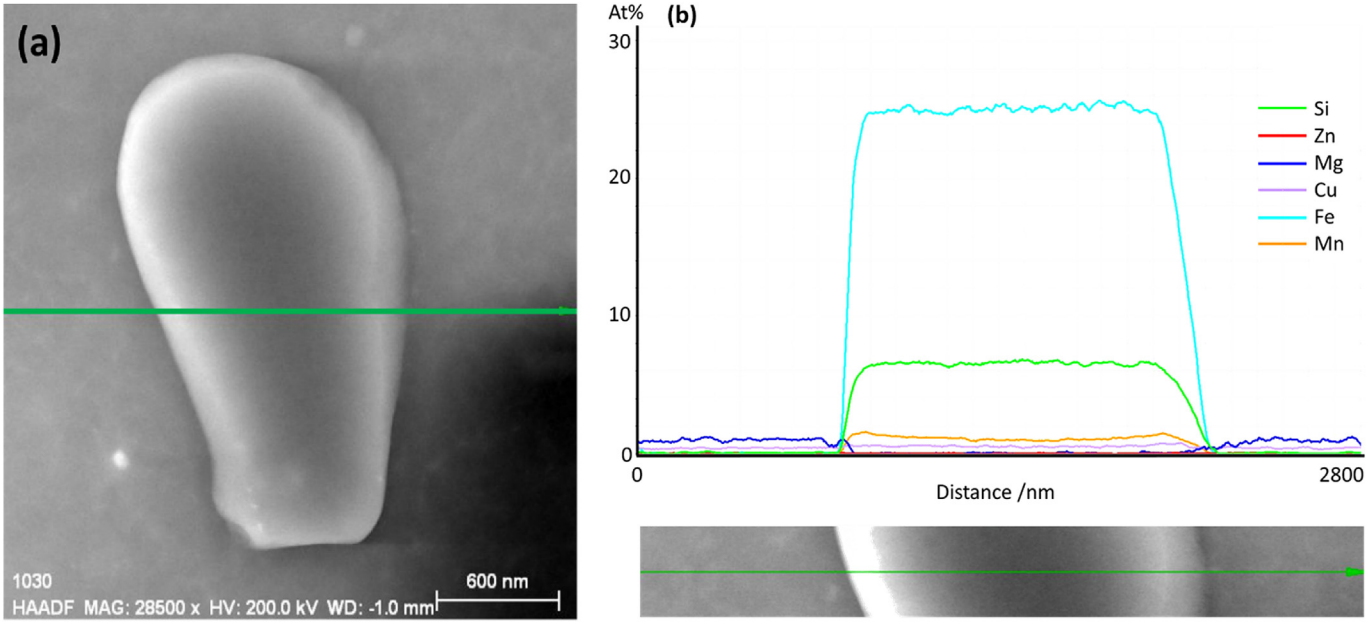

Fig. 6. STEM-HAADF image (a) and EDX linescan across a coarse particle in 6063Z sample without Al profile (b). The Al concentration is 66 at% across the particle (not shown).

documented in the literature that Cu addition in Al-Mg-Si alloys increases the susceptibility to intergranular corrosion (IGC) in acidic solutions [15,16,34–37]. For these alloys, IGC is attributed to microgalvanic coupling between cathodic grain boundary precipitates, identified as Q phase, or cathodic continuous copper-rich film along grain boundaries and the surrounding anodic matrix. Saito et al. [17] investigated Al-Mg-Si alloys containing various amounts of Zn (up to 1 wt%), but did not find any precipitates formed with Zn. However, because in their work a Cu free alloy was used, Q-phase precipitates could not have formed and Zn could in their absence obviously not have an influence on them. The authors of that paper still correlated the IGC susceptibility of the 1 wt% Zn

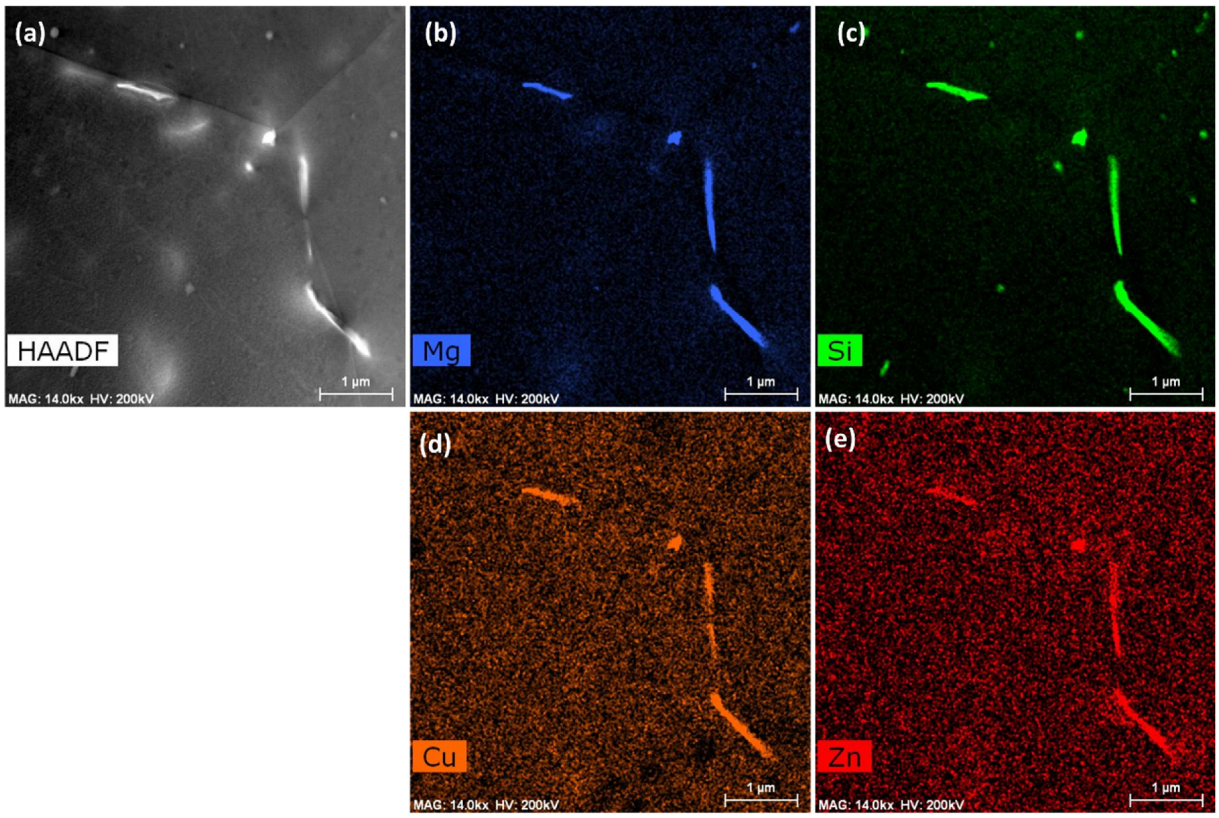

Fig. 7. STEM-HAADF image (a) and EDX elemental mappings (b to e) of a grain boundary region in 6063Z sample.

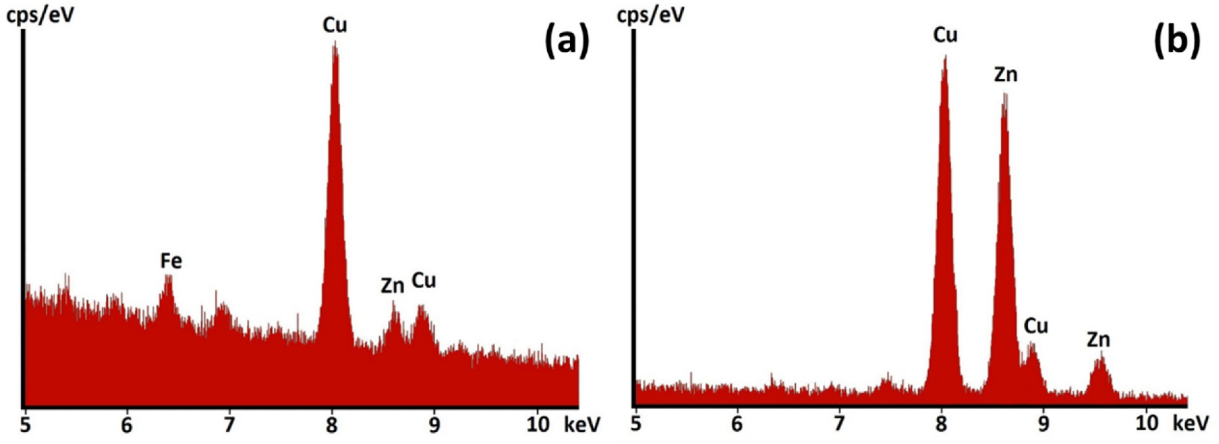

Fig. 8. EDX spectrum of a grain boundary particle in 6063 sample (a) and in 6063Z sample (b).

containing alloy with Zn segregation along grain boundaries. But at lower Zn levels like in the two investigated alloys of the present study (0.01 and 0.1 wt% vs. 0.03 vs 0.13 wt% in our alloys), no effects were reported. The IGC behavior in Al-Mg-Si alloys with additional Cu and Zn was studied by Yamaguchi and Tohma [38]. According to their macroscopic investigation, Zn addition was effective to suppress the intergranular corrosion of Al-Mg-Si-Cu alloys but their result was not correlated to any microstructural analysis. Stoknes suggested that the reduction of IGC susceptibility by Zn addition arises from a reduction of potential differences by making grain boundaries less cathodic [39]. She also proposed that if grain boundaries are enriched with metals being more active than aluminum, such as zinc, grain boundaries will act anodically. This could explain the correlation between IGC susceptibility and Zn segregation along grain boundaries observed by Saito et al. [17] in Cu free Al-Mg-Si alloys.

On the EDX maps shown in Fig. 7, no continuous Cu or Zn-rich film was detected at grain boundaries unlike what was described by Saito et al. for an alloy with higher Zn content [17]. The main difference found between the two studied alloys is that the Zn/Cu ratio in Q phase grain boundary precipitates is much higher in 6063Z alloy than in 6063 alloy. Considering that the electrochemical potential of an alloy and/or a phase depends on its composition [39–41], this might explain the effect of Cu and Zn on

the alkaline etching behavior of Cu containing 6xxx alloys. Generally, the local electrochemical potential in solution dictates whether the grain boundaries or the grains oriented in a certain direction are attacked preferentially. Because Cu increases the potential differences between the grain boundaries and the surrounding matrix by forming Q phase grain boundary precipitates, Cu boosts the grain boundary etching effect. In acidic solutions, it has been shown that an increased Cu content leads to a higher IGC susceptibility because of nobler grain boundary precipitates. Zn has a lower electrochemical potential than Cu and therefore reduces the potential of the Q phase grain boundary precipitates. Cote et al. [29], related this phenomenon with the Zn/Cu ratio, observing that if the Zn/Cu ratio is below or equal to 1 the potential of the Q phase grain boundary precipitates is cathodic enough for GBA to take place. On the other hand, if the Zn/Cu ratio is above 1, the low electrochemical potential difference of the Q phase grain boundary precipitates and the precipitation free zone and/or the grains is insignificant with respect to the potential difference between the different grain orientations leading to PGE. In our study we kept this Zn/Cu ratio similar in both alloys to study if it is really the ratio that is dominating or if also the absolute concentrations of the alloy elements are in play. It turned out that the ratio of the alloy elements in the bulk of the alloy itself is not the deciding factor, but the level of the Zn going into the Cu containing Q particles in the grain boundaries. It is thus more a microscopic than a macroscopic effect. Essentially what is important is that the Cu is needed to form the Q particles, and the higher the level of Zn (studied here to the level of 0.13 wt%), the more of it goes into those Q phases, lowering the driving forced for GBA. Unfortunately for the alloys investigated, attempts to measure these potential differences in air as well as in solution were so far unsuccessful. However, we are convinced that our hypothesis holds merit as it is additionally supported by independent observations that were even the basis for two patents stating that it is possible to prevent PGE in Al-Mg-Si-Cu-Zn alloys having a zinc content greater than 0.03 wt% if the copper content is increased [29,30]. In these patents only surface observations after alkaline etching were reported and no microstructural investigations. The present study on the other hand confirms the observations by detailed microstructure analyses, indicating that there is a systematic correlation between alkaline etching behavior and the Zn/Cu ratio in the Q grain boundary precipitates.

5. Conclusions

The microstructure and the alkaline etching behavior of two 6063 aluminum alloys in peak aged conditions were studied leading to the following conclusions:

1. Zn was found to accumulate in Q phase grain boundary precipitates.
2. At the microstructure level, the main difference between the investigated alloys was that the Zn/Cu ratio in Q phase grain boundary precipitates is much higher in the Zn rich 6063 alloy than in the Zn lean 6063 alloy, although the Zn/Cu ratio of their bulk composition is similar.
3. The 6063 alloy with a lower Zn content is preferentially attacked at grain boundaries, presumably because of a potential difference between the grain boundary (and its precipitates) and the grains. The 6063Z alloy with a higher Zn content shows a preferential attack of certain grains (PGE) because of a negligible potential difference between grain boundary and grains compared to the potential difference between differently oriented grains.
4. The present study gives an explanation why the alkaline etching behavior of Zn and Cu containing 6000 alloys can be modified by tuning the composition of the alloy, which in turn influences the composition of grain boundary precipitates.

Conflicts of interest

The authors declare that they have no conflict of interest.

Acknowledgements

The authors gratefully thank VLAIO for financial support in the framework of the RECYCAL and RECYCAL II project (Project numbers: 140710 and HBC.2017.0300) and the company E-MAX (Belgium) for discussions and providing the Aluminum samples. Linsey Lapeire acknowledges the post-doctoral grant from FWO. The authors also acknowledge the Brazilian research agencies (CAPES and CNPq) and Wallonie-Bruxelles International (WBI) for their financial support.

References

[1] P.G. Sheasby, R. Pinner, The Surface Treatment and Finishing of Aluminum and its Alloys, sixth ed., vol. 2, ASM International, 2001.
[2] H.W. Zandbergen, Structure determination of Mg5Si6 particles in Al by dynamic electron diffraction studies, Science 277 (80-.) (1997) 1221–1225, https://doi.org/10.1126/science.277.5330.1221.
[3] G.A. Edwards, K. Stiller, G.L. Dunlop, M.J. Couper, The precipitation sequence in Al–Mg–Si alloys, Acta Mater. 46 (1998) 3893–3904, https://doi.org/10.1016/S1359-6454(98)00059-7.
[4] M.A. van Huis, J.H. Chen, H.W. Zandbergen, M.H.F. Sluiter, Phase stability and structural relations of nanometer-sized, matrix-embedded precipitate phases in Al-Mg-Si alloys in the late stages of evolution, Acta Mater. 54 (2006) 2945–2955, https://doi.org/10.1016/j.actamat.2006.02.034.
[5] R. Holmestad, R. Bjørge, F.J.H. Ehlers, M. Torsæter, C.D. Marioara, S.J. Andersen, Characterization and structure of precipitates in 6xxx aluminium alloys, J. Phys. Conf. Ser. 371 (2012), 012082, https://doi.org/10.1088/1742-6596/371/1/012082.
[6] Y. Weng, Z. Jia, L. Ding, Y. Pan, Y. Liu, Q. Liu, Effect of Ag and Cu additions on natural aging and precipitation hardening behavior in Al-Mg-Si alloys, J. Alloys Compd. 695 (2017) 2444–2452, https://doi.org/10.1016/j.jallcom.2016.11.140.
[7] D.J. Chakrabarti, D.E. Laughlin, Phase relations and precipitation in Al-Mg-Si alloys with Cu additions, Prog. Mater. Sci. 49 (2004) 389–410, https://doi.org/10.1016/S0079-6425(03)00031-8.
[8] T. Saito, S. Muraishi, C.D. Marioara, S.J. Andersen, J. Røyset, R. Holmestad, The effects of low Cu additions and predeformation on the precipitation in a 6060 Al-Mg-Si alloy, Metall. Mater. Trans. A Phys. Metall. Mater. Sci. 44 (2013) 4124–4135, https://doi.org/10.1007/s11661-013-1754-3.
[9] J. Holmestad, M. Ervik, C.D. Marioara, J.C. Walmsley, Investigation of grain boundaries in an Al-Mg-Si-Cu alloy, Mater. Sci. Forum 794–796 (2014) 951–956. 10.4028/www.scientific.net/MSF.794-796.951.
[10] C. Barbosa, J.M.A. Rebello, O. Acselrad, J. Dille, J.-L. Delplancke, Identification of precipitates in 6013 aluminum alloy (Al–Mg–Si–Cu), Z. Met. 93 (2002) 208–211, https://doi.org/10.3139/146.020208.
[11] T. Saito, C.D. Marioara, S.J. Andersen, W. Lefebvre, R. Holmestad, Aberration-corrected HAADF-STEM investigations of precipitate structures in Al-Mg-Si alloys with low Cu additions, Philos. Mag. 94 (2014) 520–531, https://doi.org/10.1080/14786435.2013.857051.
[12] W. Yang, S. Ji, Z. Li, M. Wang, Grain boundary precipitation induced by grain crystallographic misorientations in an extruded Al-Mg-Si-Cu alloy, J. Alloys Compd. 624 (2015) 27–30, https://doi.org/10.1016/j.jallcom.2014.10.206.
[13] S.P. Ringer, K. Hono, Microstructural evolution and age hardening in aluminium alloys: atom probe field-ion microscopy and transmission electron microscopy studies, Mater. Char. 44 (2000) 101–131, https://doi.org/10.1016/S1044-5803(99)00051-0.
[14] C.D. Marioara, S.J. Andersen, T.N. Stene, H. Hasting, J. Walmsley, A.T.J. Van Helvoort, et al., The effect of Cu on precipitation in Al-Mg-Si alloys, Philos. Mag. 87 (2007) 3385–3413, https://doi.org/10.1080/14786430701287377.
[15] G. Svenningsen, J.E. Lein, A. Bjørgum, J.H. Nordlien, Y. Yu, K. Nisancioglu, Effect of low copper content and heat treatment on intergranular corrosion of model AlMgSi alloys, Corros. Sci. 48 (2006) 226–242, https://doi.org/10.1016/j.corsci.2004.11.025.
[16] G. Svenningsen, M.H. Larsen, J.H. Nordlien, K. Nisancioglu, Effect of high temperature heat treatment on intergranular corrosion of AlMgSi(Cu) model alloy, Corros. Sci. 48 (2006) 258–272, https://doi.org/10.1016/j.corsci.2004.12.003.
[17] T. Saito, S. Wenner, E. Osmundsen, C.D. Marioara, S.J. Andersen, J. Røyset, et al., The effect of Zn on precipitation in Al-Mg-Si alloys, Philos. Mag. 94 (2014)

2410–2425, https://doi.org/10.1080/14786435.2014.913819.
[18] M. Lableu, F. Savard, R.T. Alcan, Metallurgical assessment of acid etch as anodizing pretreatment, Anodizing Conf. Montr. (2010) 12.
[19] E.V. Koroleva, G.E. Thompson, P. Skeldon, B. Noble, Crystallographic dissolution of high purity aluminium, Proc. R. Soc. A Math. Phys. Eng. Sci. 463 (2007) 1729–1748, https://doi.org/10.1098/rspa.2007.1846.
[20] H. Habazaki, X. Zhou, K. Shimizu, P. Skeldon, G.E. Thompson, G.C. Wood, Incorporation and mobility of zinc ions in anodic alumina films, Thin Solid Films 292 (1997) 150–155, https://doi.org/10.1016/S0040-6090(96)09006-2.
[21] M.U.F. Chandia, Ø. Bauger, T. Furu, Effect of composition , grain size and texture on the etching response of 6xxx alloys, in: Proc. 12th Int. Conf. Alum. Alloy., Yokohama, 2010, pp. 781–786.
[22] A.J. Dowell, Metal Structure and Composition effects in the alkaline etching of aluminium, Trans. IMF 65 (1987) 147–151, https://doi.org/10.1080/00202967.1987.11870791.
[23] B. Holme, N. Ljones, A. Bakken, A. Lunder, J.E. Lein, L. Vines, et al., Preferential grain etching of AlMgSi(Zn) model alloys, ECS Trans. 25 (2010) 71–79, https://doi.org/10.1149/1.3496068.
[24] M. Gentile, E.V. Koroleva, P. Skeldon, G.E. Thompson, P. Bailey, T.C.Q. Noakes, Influence of grain orientation on zinc enrichment and surface morphology of an Al-Zn alloy, Surf. Interface Anal. 42 (2010) 287–292, https://doi.org/10.1002/sia.3147.
[25] Ø. Bauger, H. Bjerkaas, Aspects of preferential grain etching during alkaline pre-etching step before anodizing of aluminum profiles, in: Proc. Tenth Int. Alum. Extrus. Technol. Semin., 2012, pp. 421–430.
[26] M. Gentile, E.V. Koroleva, P. Skeldon, G.E. Thompson, P. Bailey, T.C.Q. Noakes, Influence of pre-treatment on the surface composition of Al-Zn alloys, Corros. Sci. 52 (2010) 688–694, https://doi.org/10.1016/j.corsci.2009.10.023.
[27] J. Asensio-Lozano, B. Suárez-Peña, G.F. Vander Voort, Effect of processing steps on the mechanical properties and surface appearance of 6063 aluminium extruded products, Materials (Basel) 7 (2014) 4224–4242, https://doi.org/10.3390/ma7064224.
[28] J.M.C. Mol, J. van de Langkruis, J.H.W. de Wit, S. van der Zwaag, An integrated study on the effect of pre- and post-extrusion heat treatments and surface treatment on the filiform corrosion properties of an aluminium extrusion alloy, Corros. Sci. 47 (2005) 2711–2730, https://doi.org/10.1016/j.corsci.2004.11.003.
[29] J.F. Cote, W.E. Cooke, R.C. Spooner, ALUMINUM ALLOY, US3594133, 1971.
[30] Ø. Bauger, O. Reiso, Aluminium Extrusion Alloy Suitable for Etched and Anodized Components, WO 2017093304A1, 2017.
[31] J.E. Hatch, Aluminum: Properties and Physical Metallurgy, ASM, Metals Park, OH, 1990.
[32] C.D. Marioara, S.J. Andersen, H.W. Zandbergen, R. Holmestad, The influence of alloy composition on precipitates of the Al-Mg-Si system, Metall. Mater. Trans. A Phys. Metall. Mater. Sci. 36 (2005) 691–702, https://doi.org/10.1007/s11661-005-1001-7.
[33] L. Zhen, W.D. Fei, S.B. Kang, H.W. Kim, Precipitation behaviour of Al-Mg-Si alloys with high silicon content, J. Mater. Sci. 32 (1997) 1895–1902, https://doi.org/10.1023/A:1018569226499.
[34] S.K. Kairy, P.A. Rometsch, K. Diao, J.F. Nie, C.H.J. Davies, N. Birbilis, Exploring the electrochemistry of 6xxx series aluminium alloys as a function of Si to Mg ratio , Cu content , ageing conditions and microstructure, Electrochim. Acta 190 (2016) 92–103, https://doi.org/10.1016/j.electacta.2015.12.098.
[35] M.H. Larsen, J.C. Walmsley, O. Lunder, R.H. Mathiesen, K. Nisancioglu, Intergranular corrosion of copper-containing AA6xxx AlMgSi aluminum alloys, J. Electrochem. Soc. 155 (2008) C550, https://doi.org/10.1149/1.2976774.
[36] G. Svenningsen, M.H. Larsen, J.C. Walmsley, J.H. Nordlien, K. Nisancioglu, Effect of artificial aging on intergranular corrosion of extruded AlMgSi alloy with small Cu content, Corros. Sci. 48 (2006) 1528–1543, https://doi.org/10.1016/j.corsci.2005.05.045.
[37] C. Schnatterer, D. Zander, Influence of the grain boundary chemistry on the intergranular corrosion mechanisms of a high-strength Al-Mg-Si alloy, Surf. Interface Anal. 48 (2016) 750–754, https://doi.org/10.1002/sia.5859.
[38] K. Yamaguchi, K. Tohma, Effect of Zn addition on intergranular corrosion resistance of Al-Mg-Si-Cu, in: Proceeding 6th Int. Conf. Alum. Alloy., vol. 3, 1998, pp. 1657–1662. http://www.icaa-conference.net/ICAA6/Aluminium Alloys Volume3/1657-1662.pdf.
[39] M. Stoknes, T. Furu, O. Lunder, Effect of Copper and Zinc on Corrosion Behaviour and Mechanical Properties in 6082-Alloys, 2015.
[40] T. Minoda, H. Yoshida, Effect of grain boundary characteristics on intergranular corrosion resistance of 6061 aluminum alloy extrusion, Metall. Mater. Trans. A 33 (2002) 2891–2898, https://doi.org/10.1007/s11661-002-0274-3.
[41] I.L. Muller, J.R. Galvele, Pitting potential of high purity binary aluminium alloys-II. AlMg and AlZn alloys, Corros. Sci. 17 (1977) 995–1007, https://doi.org/10.1016/S0010-938X(77)80014-0.